Explosive increase in convective Extreme El Niño events in the CO_2 removal scenario

Gayan Pathirana[1,2], Ji-Hoon Oh[1], Wenju Cai[3], Soon-Il An[1,4], Seung-Ki Min[1], Seo-Young Jo[1], Jongsoo Shin[4], Jong-Seong Kug[1,5*]

[1]Division of Environmental Science and Engineering, Pohang University of Science and Technology (POSTECH), Pohang, South Korea.

[2]Department of Oceanography and Marine Geology, FMST, University of Ruhuna, Matara, Sri Lanka.

[3]Centre for Southern Hemisphere Oceans Research (CSHOR), CSIRO Oceans and Atmosphere, Hobart, Australia.

[4]Department of Atmospheric Sciences, Yonsei University, Seoul, South Korea.

[5]Institute for Convergence Research and Education in Advanced Technology, Yonsei University, Seoul, South Korea.

[*]Corresponding authors. Email: jskug@postech.ac.kr

Professor Jong-Seong Kug, Division of Environmental Science and Engineering, Pohang University of Science and Technology, Pohang 37673, South Korea.

Supplementary Information

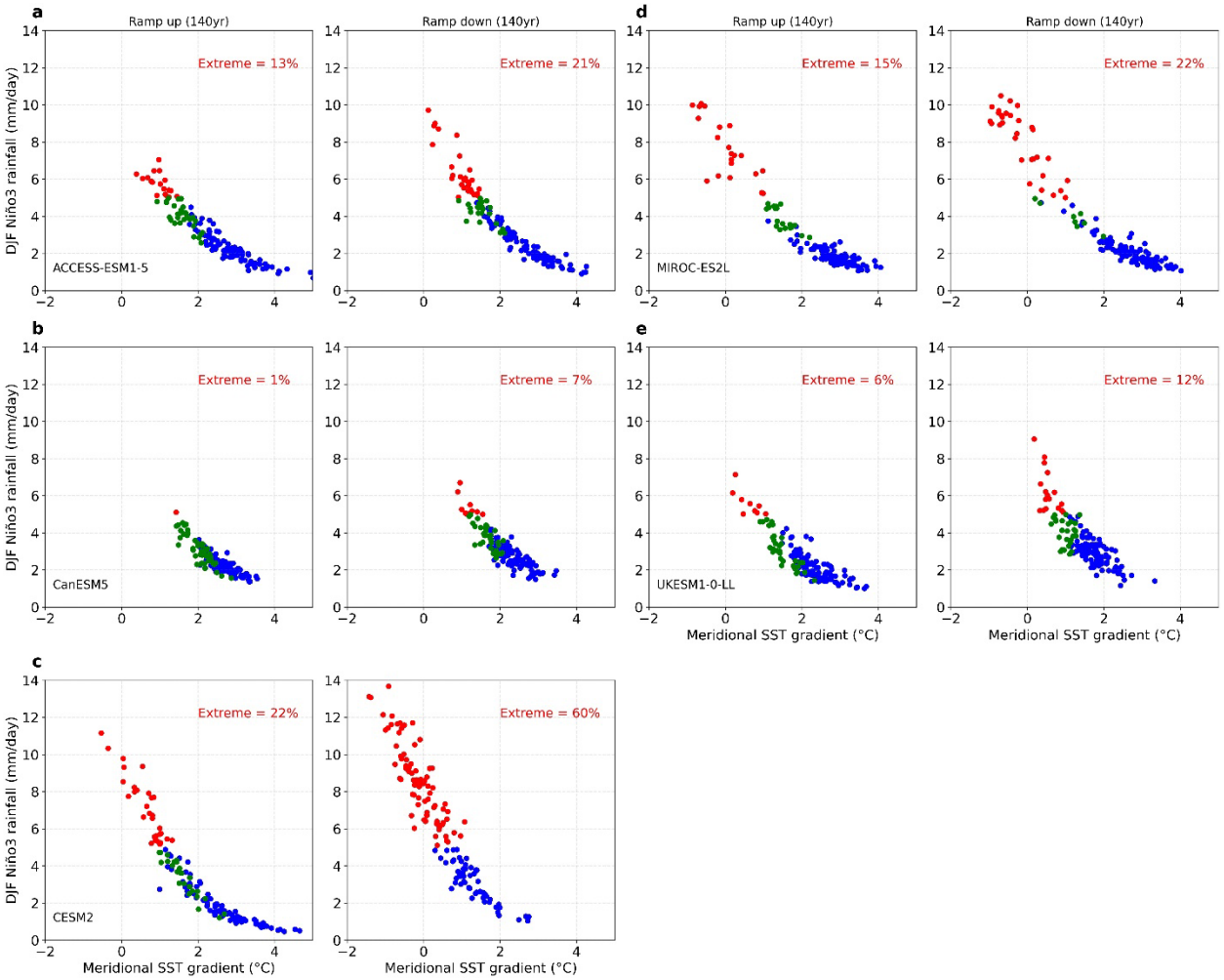

Supplementary figure 1 | Nonlinear characteristics of model convective extreme El Niño (CEE) and changes in occurrences in CMIP6. Same as Fig. 1, but for ramp-up (140 years) and ramp-down (140 years). The percentage of occurrences of CEE events in each period is shown. The data from the individual models in CMIP6 (ACCESS-ESM1-5, CanESM5, CESM2, MIROC-ES2L, UKESM1-0-LL). The models simulate a total of 80 CEE events over 700 years in the ramp-up phase and 171 events in the ramp-down phase.

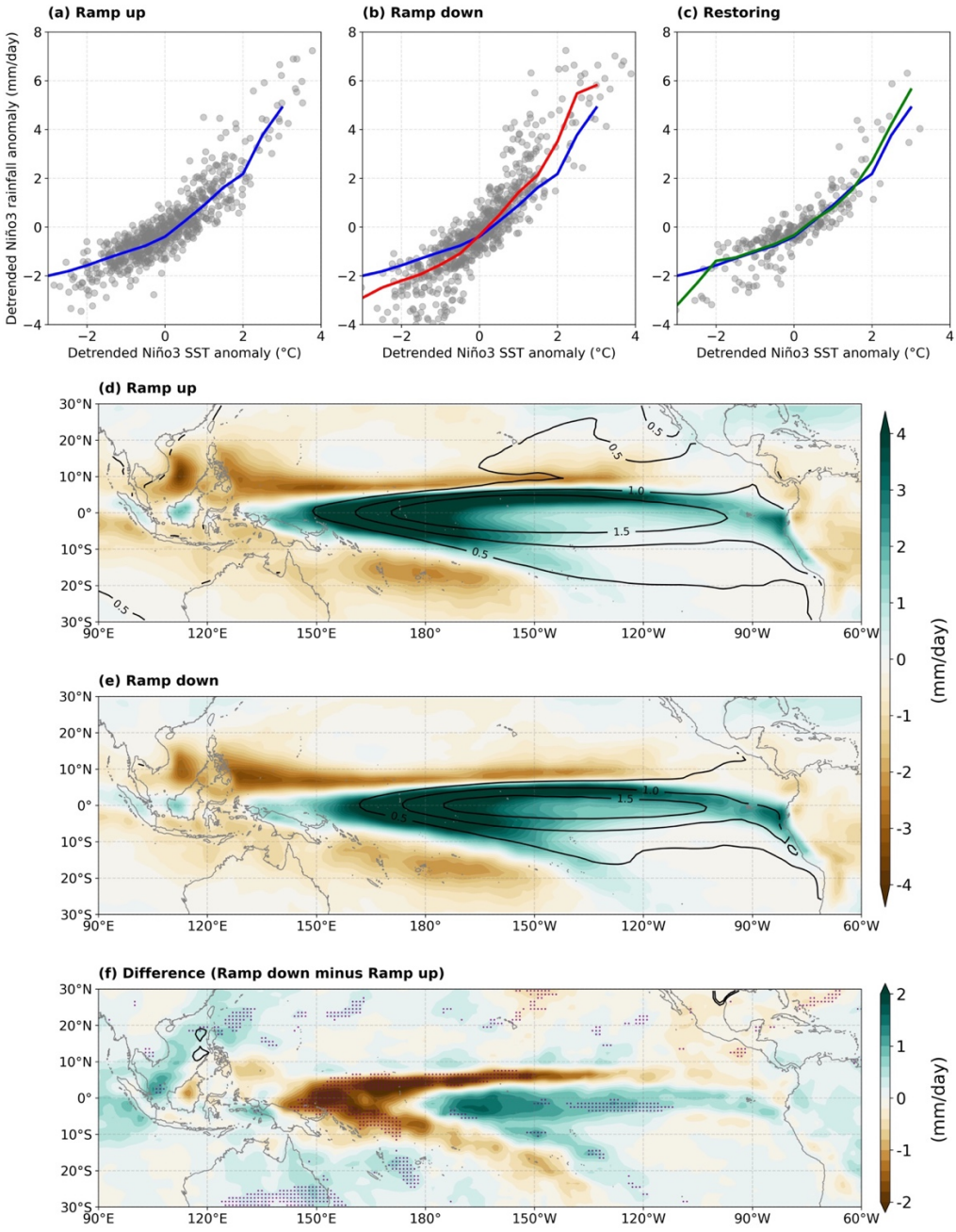

Supplementary figure 2 | Changes in Niño3 SST-rainfall relationship in CMIP6. Same as Fig. 3, but for ramp-up (140 years), ramp-down (140 years), and restoring (50 years). The data is from the MME of CMIP6 models (ACCESS-ESM1-5, CanESM5, CESM2, MIROC-ES2L, UKESM1-0-LL).

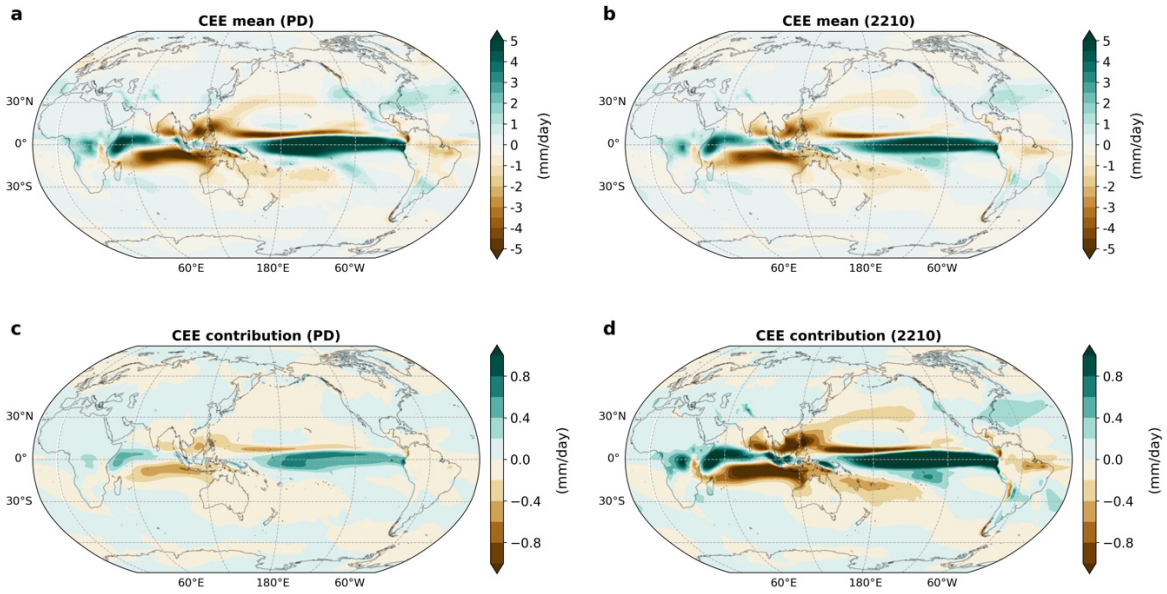

Supplementary figure 3 | Changes in the CEE precipitation. Composite of precipitation anomalies in **a)** PD, and **b)** Year 2210, during CEE. Contribution to the mean-state by CEE in **c)** PD, and **d)** Year 2210. Contribution to the mean-state is calculated as the sum of precipitation anomalies of total CEE events (i.e., 289 CEE events from 2195 to 2225) divide by the total ensemble years in each period (i.e., 28 ensembles x 31 years).

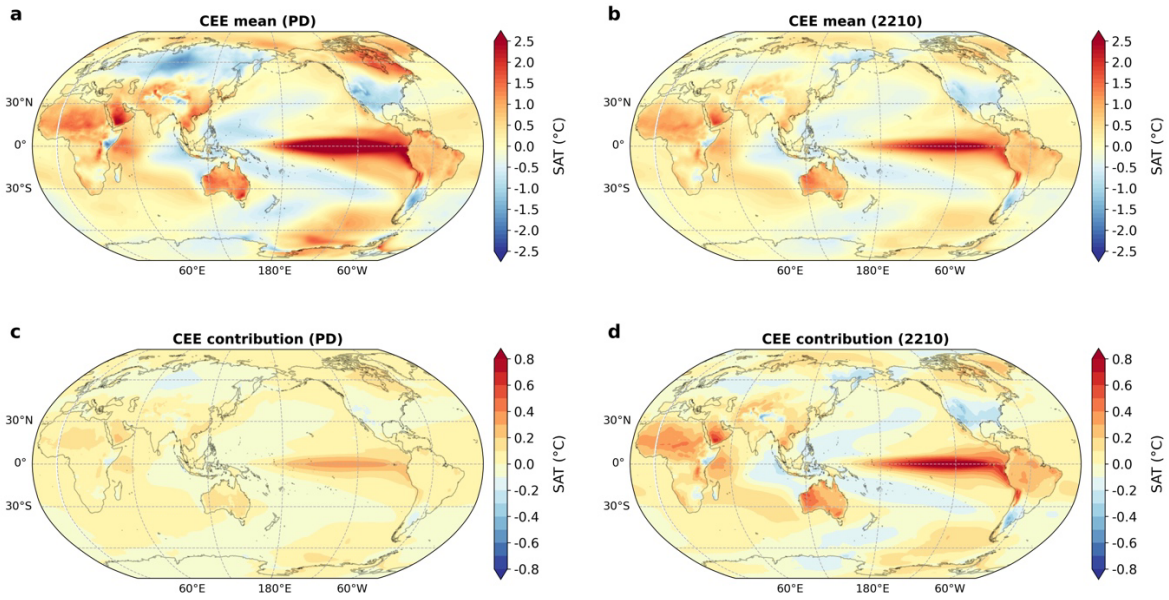

Supplementary figure 4 | Changes in the surface air temperature. Same as supplementary figure 3, but for surface temperature.

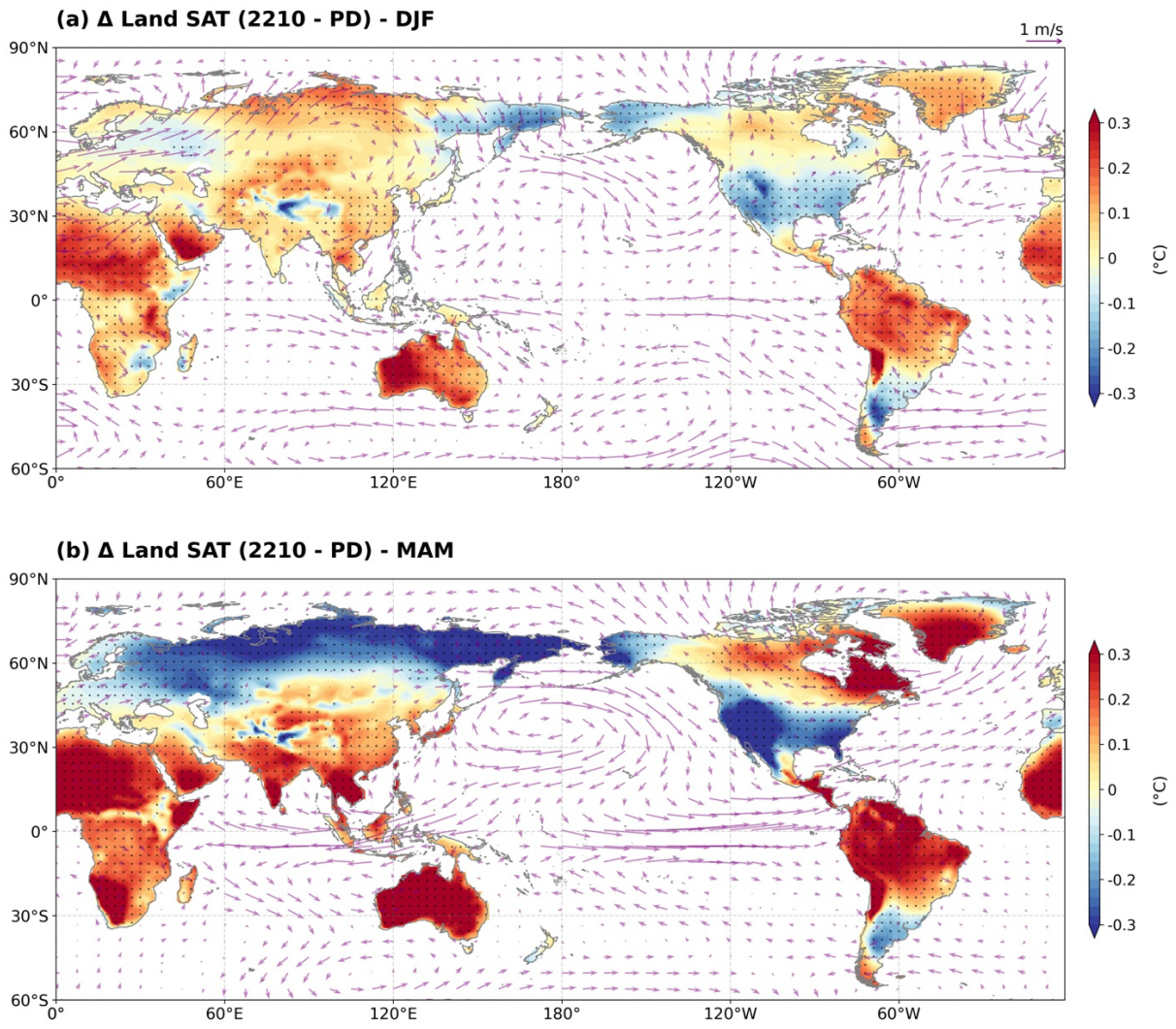

Supplementary figure 5 | Changes in the land surface temperature during CEE. Difference in the land surface temperature anomalies (shading) and 850hPa winds (vector) for **a)** boreal winter, and **b)** following spring, between Year 2210 and PD climate. The regions marked with black dots denote the significant regions at the 95% confidence interval. Difference is calculated as the contribution to the mean-state change by CEE in Year 2210 (Supplementary Fig. 4d, see methods) minus the contribution to the mean-state change by CEE in PD climate (Supplementary Fig. 4c).

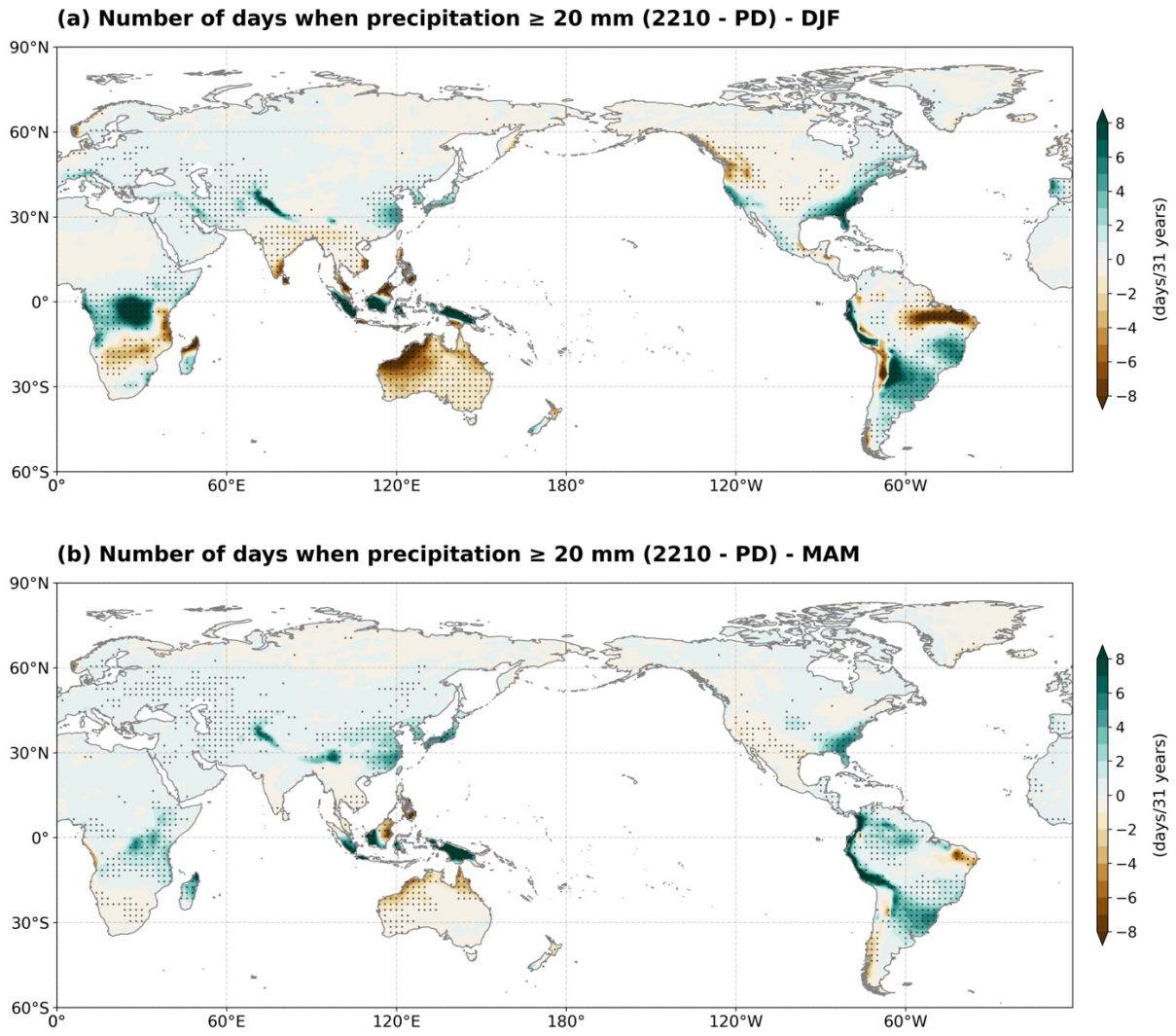

Supplementary figure 6 | Changes in the number of extreme rainy days during CEE. Difference in the number of days when precipitation >= 20 mm (shading) for **a)** boreal winter, and **b)** following spring, between Year 2210 and PD climate. The shaded regions are significant at the 95% confidence interval. Difference is calculated by taking the number of anomalous extreme precipitation days during total CEE events in Year 2210 (2195 to 2215) minus the number of anomalous extreme precipitation days during total CEE events in PD climate (see methods).